



## Microfiltration and ultrafiltration as a post-treatment of biogas plant digestates for producing concentrated fertilizers

M.S. Camilleri-Rumbau<sup>a,\*</sup>, B. Norddahl<sup>a</sup>, J. Wei<sup>b</sup>, K.V. Christensen<sup>a</sup>, L.F. Søtoft<sup>a</sup>

<sup>a</sup>Department of Chemical Engineering, Biotechnology and Environmental Technology–University of Southern Denmark, Niels Bohrs Allé 1, 5230 Odense M, Denmark, email: [mscr@kbm.sdu.dk](mailto:mscr@kbm.sdu.dk) (M.S. Camilleri-Rumbau)

<sup>b</sup>Alfa Laval Nakskov A/S, Business Centre Membranes, Stavangervej 10, 4900 Nakskov, Denmark

Received 3 March 2014; Accepted 9 November 2014

### ABSTRACT

Biogas plant digestate liquid fractions can be concentrated by microfiltration and ultrafiltration. Two types of microfiltration membranes (polysulphone (PS) and surface-modified polyvinylidene fluoride (PVDF)) were used to process digestate liquid fractions, and to assess their applicability in the recovery of particulate phosphorus, compared to an ultrafiltration membrane (polyethersulphone (PES)). Results show that membrane material, operational conditions, and pore diameter influenced the permeate flux pattern during microfiltration. The PS membranes initially had a higher tendency to foul than PVDF membranes. However, during the filtration process, as fouling built up, the permeate flux behavior of the two membranes became very similar. During the concentration of digestate liquid fractions, the microfiltration PS membrane and the ultrafiltration PES membrane achieved the highest phosphorus rejection (80% w/w), suggesting that there was a correlation between the membrane material and both the fouling trend and phosphorus rejection. A two-step basic-acidic cleaning was unable to recover the initial water flux for the fouled microfiltration membranes. In conclusion, the PS microfiltration membranes might be a good strategy for recovering phosphorus from digestate liquid fractions. Further research leading to adequate cleaning procedures, for microfiltration PS and PVDF membranes treating digestate liquid fractions though, are needed.

*Keywords:* Microfiltration; Ultrafiltration; Digested manure; Polysulphone (PS); Polyvinylidene fluoride (PVDF); Polyethersulphone (PES); Phosphorus recovery; Zeta potential

### 1. Introduction

Livestock production has increased dramatically in the last decades due to an increased consumption in meat and an increase in the human population [1]. As

large centralized livestock production leads to large production of manure, centralized biogas production by anaerobic digestion is of growing interest as a green energy solution in areas with industrialized livestock production. Anaerobic digestion stabilizes and converts about 20–25% of the organic matter present in animal manure into biogas; it is considered

\*Corresponding author.

Presented at IMSTEC 2013–8th International Membrane Science and Technology Conference, Organized by the Membrane Society of Australia, 25–29 November, 2013, Melbourne, Australia

a reliable source of bioenergy and it minimizes greenhouse gas emissions and odors [2–4]. Anaerobic digestion mineralizes some of the organic nitrogen and increases the  $\text{NH}_3/\text{NH}_4^+$  content by about 15%. The same occurs with the organic phosphorous, the concentration of which in the inorganic form also increases after anaerobic digestion [4]. Digestates contain large amounts of nutrients in the form of nitrogen, phosphorus, potassium, organic matter, and micronutrients (e.g. calcium, chloride, sodium, copper, zinc, manganese, etc.) [5]. It is a common practice to use digestates as a fertilizer source and to spread the resulting liquid fraction after solid–liquid separation on the fields [6]. However, this can lead to environmental problems mostly related to ammonia volatilization as well as surface and groundwater eutrophication [1,7]. Moreover, digestates present an unbalanced distribution of nutrients with respect to crop uptake and demand, which makes their application, as reliable fertilizers, difficult.

When digestates from centralized biogas plants are applied as fertilizer to fields far away from the biogas plant, it is advantageous to separate digestate in a solid fraction rich in phosphorus and a liquid fraction rich in nitrogen and potassium [8], but low in phosphorus. Separation in a solid and liquid fraction both reduces transportation costs and makes it possible to obtain a more balanced fertilizer composition. Traditionally, this separation is done using either a decanter centrifuge or a screw press. The obtained liquid fractions though, are still dilute in nitrogen and potassium and further concentration of these nutrients is necessary [1]. Moreover, the concentration of particulate phosphorus present in the liquid fraction might be increased by concentration of the particulate dry matter (DM) or total solids content. It is estimated that 20% of the phosphorus in digestates is present in the fraction below  $0.45\ \mu\text{m}$ , while the remaining 30% has been found in particulates larger than  $10\ \mu\text{m}$ . Especially, the particle range between  $0.45$  and  $10\ \mu\text{m}$ , is of interest as it is the fraction that contains approximately 50% of the total phosphorus in the digestate [1,9].

Several studies have already proved that membrane separation is suitable for concentrating digestate liquid fractions [2,10–12]. Microfiltration has proved to be a reliable technique for treating digestate liquid fractions and removing suspended solids from the liquid stream [10]. Ultrafiltration has also proved to be suitable for further removal of suspended solids and colloids [12]. However, there are only few studies on microfiltration and ultrafiltration of digestate liquid fractions with special focus on the influence of membrane material, operating conditions,

and pore size on membrane fouling and phosphorus recovery [11–17]. In this study, the fouling tendency of polysulphone (PS) and surface-modified polyvinylidene fluoride (PVDF) membranes was investigated. The influence of membrane surface hydrophilicity on membrane fouling has previously been studied by Wei et al. [18]. They showed that, during filtration of bovine serum albumin (BSA), membranes made of hydrophobic materials such as PS or polyethersulphone (PES) caused severe fouling compared to membranes made of more hydrophilic surfaces (e.g. surface modified PVDF). Beier et al. [19] investigated the effect of static adsorption during ultrafiltration of an amylase enzyme solution. They found that the PES membrane had a larger static adsorption of macromolecules, due to its hydrophobic nature, than the surface-modified PVDF. Other studies, focused on the influence of the ionic strength and solution pH on the adsorption of proteins on membrane surfaces. For instance, Bayramoglu et al. and Li et al. [20,21] found that proteins with opposite surface charge, compared to that of the membrane, presented the strongest adsorption. Li et al. also found [21] that although convective forces tended to increase the amount of foulant accumulated near the membrane surface; electrostatic interactions played a stronger role which was evident from the resulting irreversible foulant adsorption. Thus, controlling the electrostatic interactions could reduce adsorption of foulants onto the membrane and consequently reduce long-term membrane fouling.

Membrane surface charge has been used as a parameter for investigating the membrane fouling tendency during ultrafiltration of silica particles [22] and during microfiltration of egg protein [23], chlorolignin, and whey protein [24] among other studies mentioned by Deshmukh and Childress [25]. However, the majority of these studies only involved rather limited solution chemistries and none of them were related to filtration of digestate liquid fractions. It has though been shown that when microfiltration membranes are used in ammonia removal for pig slurry by membrane distillation, the surface charge influences fouling [26]. Therefore, investigating the effect of surface charges of the membrane–digestate liquid fraction system is relevant to understand better the fouling mechanism in these types of membrane-based processes. This can be done by monitoring the electrostatic interaction between membrane and foulant [27,28]. The most common technique for evaluating the membrane surface charge is by streaming potential [27,29]. The zeta potential, estimated from the Helmholtz–Smoluchowsky equation from the streaming potential, has been used as

an index of the surface charge and applied during the characterization of membrane materials [27,29,30], although it is used in terms of apparent or observed zeta potential, as the Helmholtz–Smoluchowsky equation neglects the effect of surface conductance. The observed zeta potential thus becomes a preliminary diagnostic tool to identify a potential cause of membrane fouling [25].

In this study, the fouling tendency of surface-modified PVDF and PS membranes was investigated based on the observed zeta potential and operational conditions in order to evaluate the interaction between the membrane material and the feed. Phosphorus rejection during membrane filtration was also investigated. As an alternative to phosphorus recovery by microfiltration, the usage of a commercial setup combining ultrafiltration directly with an anaerobic digester was also introduced. However, the study of the fouling characteristics and filtration performance of the ultrafiltration system is only included for comparison. It is not the objective of this paper.

## 2. Materials

### 2.1. Biogas plant digestates

Microfiltration experiments were carried out on the anaerobic digestate liquid fraction from Fangel Biogas (Odense, Denmark). The feed to the anaerobic digester consisted of approximately 50% of pig slurry, 15% cattle manure, 10% chicken manure, and 25% food waste. The anaerobic digestion was mesophilic (39–40°C) and the hydraulic retention time was 30 d. The final digestate was centrifuged via a decanter centrifuge (AD-1220, GEA Westfalia, Germany). The obtained solid fraction is normally composted, while the liquid fraction is distributed to local farmers and used as a liquid fertilizer. Fangel biogas plant treats 260

tonnes·d<sup>-1</sup> of animal slurry and 60 tonnes·d<sup>-1</sup> of industrial food waste. This allows an annual energy production of 16–18 million kWh year<sup>-1</sup>. The digestate liquid fraction obtained after centrifugation was sieved using a two-step manual sieve (Retsch 5657, Germany) of 350 and 125 µm mesh size. The resulting sieved liquid fraction was used as feed to the microfiltration unit. The composition and characteristics of the digestate liquid fraction used as feed to the microfiltration system are shown in Table 1.

The ultrafiltration experiments were carried out at Bioscan A/S' anaerobic digester ultrafiltration pilot plant at mesophilic conditions (35°C) and at a hydraulic retention time of 12 d. The concentrate was recirculated to the digester [13]. The digestate had a pH value of 8 and a composition of 3.2% total solids; 2.7 (g L<sup>-1</sup>) of total ammoniacal nitrogen (TAN); and 0.53 g L<sup>-1</sup> of phosphorus and 0.46 g L<sup>-1</sup> of potassium.

### 2.2. Filtration setups

#### 2.2.1. Microfiltration unit

The microfiltration experiments were carried out on a LabStak<sup>®</sup> M10 laboratory plant (Alfa Laval, Denmark) (Fig. 1). The M10 is a cross-flow filtration module with an active membrane area of 0.036 m<sup>2</sup> which can accommodate four flat-sheet membranes (see Table 2). The laboratory plant had three M10 membrane modules placed in parallel. This made it possible to test three different membrane pore sizes at nearly identical operational conditions. The feed was pumped from one shared 15 L-feed tank through an external spur gear pump (GC6-KDT-KKU, Pulsafeeder Inc. USA) with a maximum flow rate of 2.8 m<sup>3</sup> h<sup>-1</sup>. Piping and connections in the plant were made of stainless steel AISI 316. The inflow velocity to the microfiltration module was measured through a

Table 1  
Composition of Fangel Biogas Plant digestate liquid fraction

Parameter	Fangel Biogas digestate liquid fraction (used for microfiltration experiments)
pH	8.1–8.3
Dry matter (DM) (%)	2.7
Total kjeldahl nitrogen (TKN) (g L <sup>-1</sup> )	3.4
Total ammoniacal nitrogen (TAN) (g L <sup>-1</sup> )	3.15
Total phosphorus (TP) (g L <sup>-1</sup> )	0.46
Potassium (K <sup>+</sup> ) (g L <sup>-1</sup> )	2.03
Calcium (Ca <sup>2+</sup> ) (g L <sup>-1</sup> )	0.59
Magnesium (Mg <sup>2+</sup> ) (g L <sup>-1</sup> )	0.09
Sodium (Na <sup>+</sup> ) (g L <sup>-1</sup> )	1.28

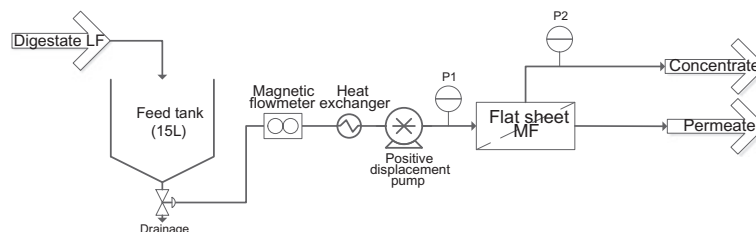


Fig. 1. LabStak® microfiltration M10 setup.

Table 2  
Membrane materials and experimental conditions during microfiltration experiments

ITEM	Microfiltration parameters
Membrane type	Flat sheet membranes
Membrane materials	Surface modified PVDF and PS
Manufacturer	Alfa Laval, Denmark
Mean pore diameters ( $\mu\text{m}$ )	0.2 (membrane types PVDF2, PS2) 0.5 (membrane types PVDF5, PS5) 0.8 (membrane types PVDF8, PS8)
Membrane area ( $\text{m}^2$ )	0.144
Operating transmembrane pressures (bar)	1 and 1.5
Feed flow ( $\text{L h}^{-1}$ )	800 and 1,040
Operating feed cross flow velocity ( $\text{m s}^{-1}$ )	1.1 and 1.4
Operating temperature ( $^{\circ}\text{C}$ )	30

digital flowmeter (IFS1000 K, Krohne Altometer, Germany) and the transmembrane pressure, by analog pressure gauges (P1 and P2 in Fig. 1) (Tempress, Denmark). The temperature was controlled through a multi-tube heat exchanger (Alfa Laval, Sweden). All

the experiments were run at  $30^{\circ}\text{C}$ , chosen as a relevant temperature for mesophilic digestate liquid fractions obtained after digestate centrifugation.

### 2.2.2. Ultrafiltration unit

The ultrafiltration experiments were performed by Bioscan A/S (Denmark) at the pilot plant shown in Fig. 2, equipped with PES tubular membranes (STUF 2.5/1.7 AL (S) 719, Membratex, South Africa) having an active area of  $7.1 \text{ m}^2$  and a cut-off of 40 kDa. The system was run at 1.5–3.5 bar and cross-flow velocities of 2, 2.6, 2.9, and  $4.3 \text{ m s}^{-1}$ . The anaerobic digester was fed with screw press pre-treated slurry from a pig farm. The digestate was produced in the 150 L-pilot-scale digester tank. The digestion temperature was kept constant at  $35^{\circ}\text{C}$  by an external heating system. All pipings were made of AISI 304 stainless steel. The digested biomass was separated and treated subsequently by tubular ultrafiltration membranes. The digestate velocity to the UF module was controlled by a calibrated screw pump (Mono S32M, Mono Pumps, UK) with a VLT® frequency converter (Danfoss, Denmark). The bulk of the ultrafiltration permeate was recirculated into the digester in order to keep the liquid level constant in the digester [14].

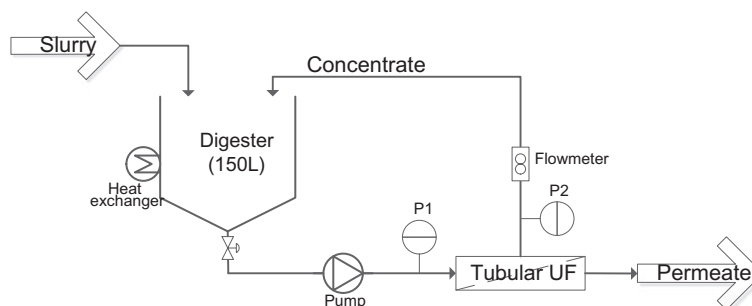


Fig. 2. Ultrafiltration pilot plant setup.

### 3. Methods

#### 3.1. Microfiltration experimental procedure

Two membrane materials (surface-modified PVDF and PS) and three pore sizes (0.2, 0.5, and 0.8  $\mu\text{m}$ ) were tested (Table 2). The PVDF membrane surface was modified by the manufacturer to increase its hydrophilicity. Fresh membranes were used for each experimental run. Membrane pre-cleaning and conditioning was done with a 0.1% w/w solution of Ultrasil 10 (Henkel, Germany) at 50°C recirculated for 30 min.

The feed was run at constant feed velocities of 1.1 and 1.4  $\text{m s}^{-1}$  and constant transmembrane pressures of 1.0 and 1.5 bar. The feed temperature was kept at 30°C throughout the entire set of experiments. Before starting a filtration cycle, clean water tests were performed on the fresh membranes, using deionized water, at the same operational conditions as the related filtration experiment. Each filtration experiment lasted 3–4 h. After the filtration run and membrane flushing, a clean water test was performed in order to compare the permeate flux before and after filtration of the digestate liquid fraction. Then the membranes were chemically cleaned. The cleaning procedure was a sequence of a basic cleaning using a 0.1 M NaOH solution (pH  $12.1 \pm 0.1$ ), followed by an acidic cleaning using 0.1 M citric acid solution (pH  $2.2 \pm 0.1$ ). Each cleaning was conducted for 30 min at 30°C. In between the basic and acidic cleaning cycles, clean water tests were performed to check the membrane flux recovery after each chemical cleaning step. The cleaning procedure was done at the same operational conditions as the corresponding filtration experiments.

#### 3.2. Surface characterization of membranes and materials

##### 3.2.1. Surface charge of particulate matter in Fangel Biogas digestate and microfiltration fractions

The observed zeta potential of the Fangel Biogas digestate, concentrate, and permeate fractions after microfiltration was obtained using Electrophoretic Light Scattering (Zetasizer Nano, Malvern, UK). The sample dispersant was deionized water and the analysis temperature was 25°C. The scattering angle was 12.8° and the samples were analyzed in a disposable Z-dip cell. The zeta potential calculation from experimental electrokinetic data follows the Helmholtz–Smoluchowski equation. All the samples required dilution. The observed zeta potential and standard deviation were reported as an average of at least 12 readings. Measurements were done in triplicate.

##### 3.2.2. Surface charge of microfiltration PVDF and PS membrane surfaces

A SurPASS adjustable gap cell (Anton Paar, Austria) for small rectangular pieces of planar samples was used to obtain the observed zeta potential by measuring the streaming potential of the PS and PVDF membrane samples. Prior to the measurements, membrane samples were cleaned to remove the glycerine-protective coating on the membrane surface. 0.03 wt% NaOH was used for pre-treating PVDF membranes and 0.3 wt% NaOH was used for PS membranes. The membrane samples were fixed on the sample holders with double-sided adhesive tape. The cell gap, where two pieces of the  $2 \times 1$  mm membrane sample were attached, had a height of 0.1 mm. Before performing the first measurement, the complete electrolyte circuit was rinsed with deionized water. A 500 mL solution of 1 mM NaCl was used as electrolyte and the pressure drop along the gap was set at 300 mbar [28]. The pH was controlled by adding HCl 0.1 M and NaOH 0.1 M to the 1 mM NaCl feed solution. The streaming potential per unit pressure, through and on the membrane surface, was evaluated at a constant  $\text{Cl}^-$  concentration of 1 mM with a gradual substitution of protons by  $\text{Na}^+$  [31].

#### 3.3. Analytical methods

##### 3.3.1. Chemical analysis

During the microfiltration experiments, the pH was measured with a pHM83 pHmeter (Radiometer Analytical, France). The DM or total solids content was measured with a HG63 Halogen Moisture Analyzer (Mettler Toledo, Sweden). TKN and TAN were measured by the Kjeldahl method [32] using a Tecator Digester block and a Kjeltac Distillation unit (Foss, Denmark). Values for phosphorus, potassium, calcium, magnesium, sodium, and chlorine were analyzed by ICP-OES (ICAP 6500 Duo, Thermo Scientific, USA). For the ICP-OES analysis, 0.1 g of each sample was weighed and introduced in a digestion Teflon tube of an Ultraclave Microwave Digester (Milestone Inc., USA), and acidic digestion was allowed by adding 4 mL of  $\text{HNO}_3$  PA-ISO 69% and 1 mL of  $\text{H}_2\text{O}_2$  33% to the digestion tube. The temperature was set to increase from room temperature to 220°C over a period of 20 min. Once the samples were cooled down, the digestion Teflon tubes were filled up to 25 mL with deionized water (Merck Millipore, Germany) and the samples were analyzed by ICP-OES.



### 3.3.2. Data analysis

Microfiltration data are presented in terms of relative permeate flux, i.e. the absolute permeate flux related to the initial water flux for each tested membrane ( $J/J_0$ ) (Eq. 1). The reasoning behind this is that new fresh membranes were used for each experimental run and a high standard deviation of the related clean water fluxes was observed due to variations during membrane production. This makes it difficult to carry out a direct water flux comparison between different operational conditions. By treating the data as relative permeate fluxes, data are standardized and a direct comparison among the obtained values during the microfiltration experiments can be done.

$$\text{Relative permeate flux} = \frac{J}{J_0} \quad (1)$$

where  $J$  ( $\text{L m}^{-2} \text{h}^{-1}$ ) is the permeate flux and  $J_0$  ( $\text{L m}^{-2} \text{h}^{-1}$ ) is the initial water flux obtained for each fresh membrane before starting the filtration experiment. To compare the relative permeate fluxes of paired experiments, scatter plots are used. The time trace line generated is compared to the identity line  $y = x$ . If the relative permeate fluxes or the effect of experimental conditions on the relative permeate fluxes are identical, the time trace line should fall approximately along the identity line. Linear interpolation between data points was used to compare relative fluxes at the same processing time when experimental data were not available.

## 4. Results and discussion

### 4.1. Determination of the surface charge of liquid fractions and microfiltration membranes

The composition of the polymeric membrane-active layer influences the surface charge density of the membrane. The same applies for the particulates of the Fangel Biogas digestate liquid fraction, concentrate, and permeate obtained from the microfiltration. As membrane foulant interactions are a major issue during microfiltration of particulate liquid samples [22], such as digestate liquid fractions, the observed zeta potential of PVDF (PVDF2 and PVDF5) and PS membranes (PS2 and PS5) was measured as a function of pH. This is crucial for understanding the acid–base properties of membrane surface functional groups. Measuring the observed zeta potential of the feed as well as for the obtained concentrates and permeates (Table 3) would help to elucidate the interaction between the foulant and the microfiltration membrane surfaces.

Table 3 presents the observed zeta potential of the feed, concentrate, and permeate samples obtained during concentration experiments using PS5 and PVDF5. The typical pH of biogas plant digestates is 8–8.5. All samples were measured at a pH of  $8.2 \pm 0.1$ , to simulate the typical feed pH. All the tested samples had a zeta potential between  $-18.2$  and  $-14.7$  mV. These negative zeta potential values at high pH are most likely related to the amino and carboxyl groups present in the proteins of the analyzed samples and only to a smaller degree to the charge of the solids [33]. This might explain why feed, concentrate, and permeate show similar zeta potentials, as proteins are not expected to be separated to a significant degree by microfiltration.

Fig. 3 presents the zeta potential measurements for PVDF and PS membranes as a function of the solution pH. For the studied pH range, the PS membranes showed a significantly less negative zeta potential than the surface-modified PVDF membranes. In the pH range of interest, for the membrane feed (pH 8–8.5), both PS and PVDF membrane materials showed stable values of observed zeta potentials being  $-18.2$  mV and  $-16.0$  for PVDF2 and PVDF5, respectively; and  $-6.9$  and  $-7.1$  mV for PS2 and PS5, respectively. The initial properties of the membranes suggest that foulants might get more attracted to the PS membrane surface rather than to the PVDF membrane as the feed has an observed zeta potential of about  $-18$  mV at a basic pH (Table 3). As the difference in charge is larger between foulants and the PS than for the PVDF membrane, the PS membrane is thus less repulsive to foulants, initially.

### 4.2. Microfiltration of digestate liquid fraction during full recycling experiments

#### 4.2.1. Water test on microfiltration membranes

Water tests were conducted on fresh membranes prior to each filtration experiment (Table 4). As expected, flux increased with the applied transmembrane pressure following Darcy's law. However, a large difference between each new membrane was observed, making conclusions based on the clean water flux alone difficult. The influence of the cross-flow velocity was unclear although during water tests, this should not have a high impact (i.e. absence of fouling). It is characteristic for all water tests except, perhaps, for the PS5, that the increase in cross-flow velocity leads to a lower flux at a similar transmembrane pressure. Differences in membrane compaction cannot be the cause as both transmembrane pressure and cross-flow velocity were maintained constant and

Table 3

Observed zeta potential for samples obtained during concentration experiments reaching a VRF of 0.5 approximately (SD: standard deviation)

Sample	Membrane type	Membrane material and mean pore diameter ( $\mu\text{m}$ )	Dilution	Observed zeta potential <sub>average</sub> $\pm$ SD (mV)
Feed			1:50	$-18 \pm 6$
Concentrate	PVDF5	PVDF 0.5	1:100	$-15 \pm 6$
Concentrate	PS5	PS 0.5	1:50	$-15 \pm 6$
Permeate	PVDF5	PVDF 0.5	1:50	$-17 \pm 7$
Permeate	PS5	PS 0.5	1:50	$-16 \pm 7$

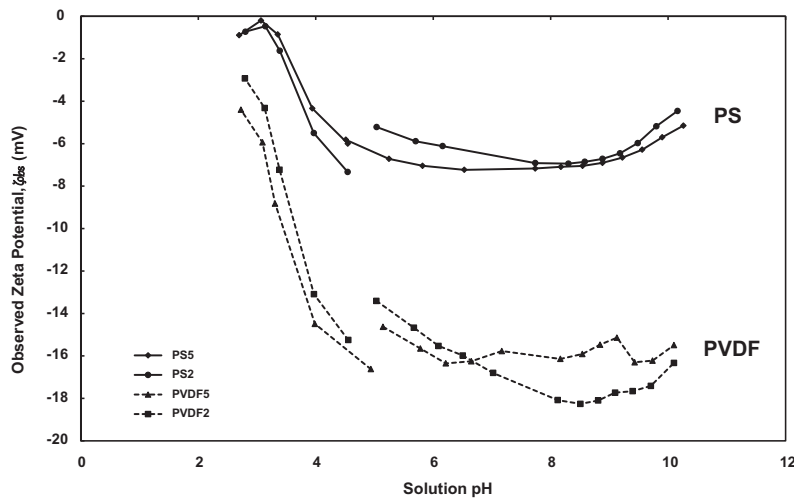


Fig. 3. Observed zeta potential as a function of solution pH for PVDF2 and PVDF5, PS2 and PS5 fresh membranes (zeta potential calculated as streaming potential per unit of applied pressure on the membrane; each point represents a slope for a linear representation with a correlation better than 0.95).

Table 4

Water flux values for PVDF and PS membranes as a function of transmembrane pressure ( $\Delta P$ ) (1 and 1.5 bar) at different cross-flow velocities (1.1. and 1.4  $\text{m s}^{-1}$ )

Conditions		Membrane type					
$v$ ( $\text{m s}^{-1}$ )	$\Delta P$ (bar)	Water flux ( $\text{L m}^{-2} \text{h}^{-1}$ ) $\times 10^3$					
		PVDF2	PVDF5	PVDF8	PS2	PS5	PS8
1.4	1.50	2.27	1.38	2.63	0.65	1.51	1.02
1.4	1.00	1.13	0.95	0.96	0.31	0.55	0.52
1.1	1.50	2.50	1.35	2.94	0.61	1.28	1.41
1.1	1.00	2.17	1.19	2.27	0.32	0.76	0.70

the transmembrane pressure did not increase with increasing cross-flow velocity. Due to these variations in clean water fluxes between each new documented membrane, results during microfiltration of digestate liquid fractions were evaluated in terms of relative permeate fluxes following Eq. (1).

4.2.2. Microfiltration performance: Effect of operational conditions, material interaction and membrane pore size

Fig. 4 presents the permeate fluxes with experimental time obtained for the studied PVDF and PS membranes during microfiltration of digestate liquid

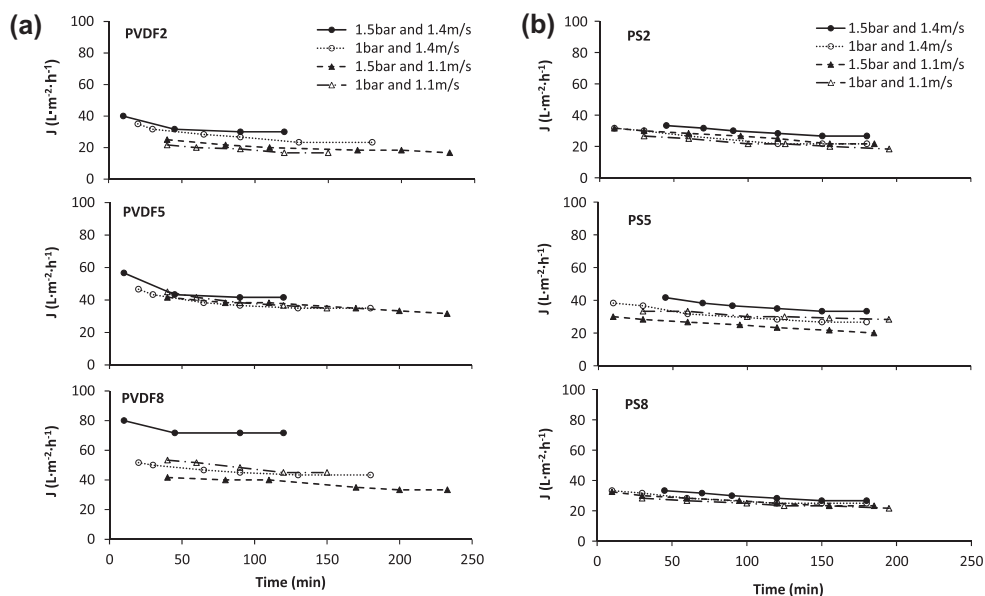


Fig. 4. Permeate flux during microfiltration experiments as a function of operational time using (a) PVDF membranes and (b) PS membranes.

fractions. As can be observed, for the two PVDF and PS membranes, the obtained permeate fluxes are very low compared to the clean water fluxes (Table 4) for the same testing conditions. Moreover, a severe permeate flux decline is observed immediately during the start-up of the filtration cycle. This behavior has been reported previously to be caused by both concentration polarization and fouling on the membrane surface [19], which are especially severe when treating digestate liquid fractions. An increase in the feed cross-flow velocity during microfiltration also increased the permeate flux for all membranes. This might indicate the formation of concentration polarization and a reversible fouling layer that could be removed when increasing turbulence at the membrane surface [34]. Furthermore, the combination of a higher pressure (1.5 bar) and lower cross-flow velocity ( $1.1 \text{ m s}^{-1}$ ) resulted in the lowest permeate fluxes for all membranes probably due to a significant increase in the fouling layer resistance. This behavior is most likely caused by an increasing compression of the fouling layer, as suggested by Razi et al. [34], as increasing the cross-flow velocities to  $1.4 \text{ m s}^{-1}$  did not lead to the same relative flux as measured at 1 bar.

The relative permeate fluxes ( $J/J_0$ ), to compare the effect of membrane material and pore diameter during microfiltration using the two PS and PVDF membranes, were plotted against each other in scatter plots (Figs. 5–7). These plots mostly give information about the effect of operational conditions on the

relative permeate flux pattern. The reason why the relative permeate flux for PS is higher than the ones for PVDF is basically due to the higher clean water flux values obtained for PVDF membranes.

The impact of the operational conditions, i.e. applied pressure and cross-flow velocity, on the relative permeate fluxes for the same pore size, for the two PS and PVDF membranes can be observed in the individual graphs in Fig. 5(a)–(c). The relative permeate flux achieved with the PS membranes was generally higher than that obtained when using the PVDF membranes for a similar filtration time (i.e. the time trace lines lay beneath the identity line). However, it can be observed that the relative permeate flux decay with time was more pronounced for PS membranes than for PVDF membranes for all the membrane pore sizes. The application of a higher pressure also affected the relative permeate flux of the PS membranes more negatively than the PVDF membranes, and enhanced the reduction of the relative permeate flux most probably due to an increasing compression of the fouling layer, especially for the smaller membrane pore sizes (i.e. 0.2 and  $0.5 \mu\text{m}$ ). The combination of low pressures and high velocities appeared to be beneficial for all membranes. It also seems that the larger the membrane pore size, the smaller the effect of the material interaction, which causes an ultimate similar permeate relative fluxes for all the PS and PVDF membranes (Fig. 4).



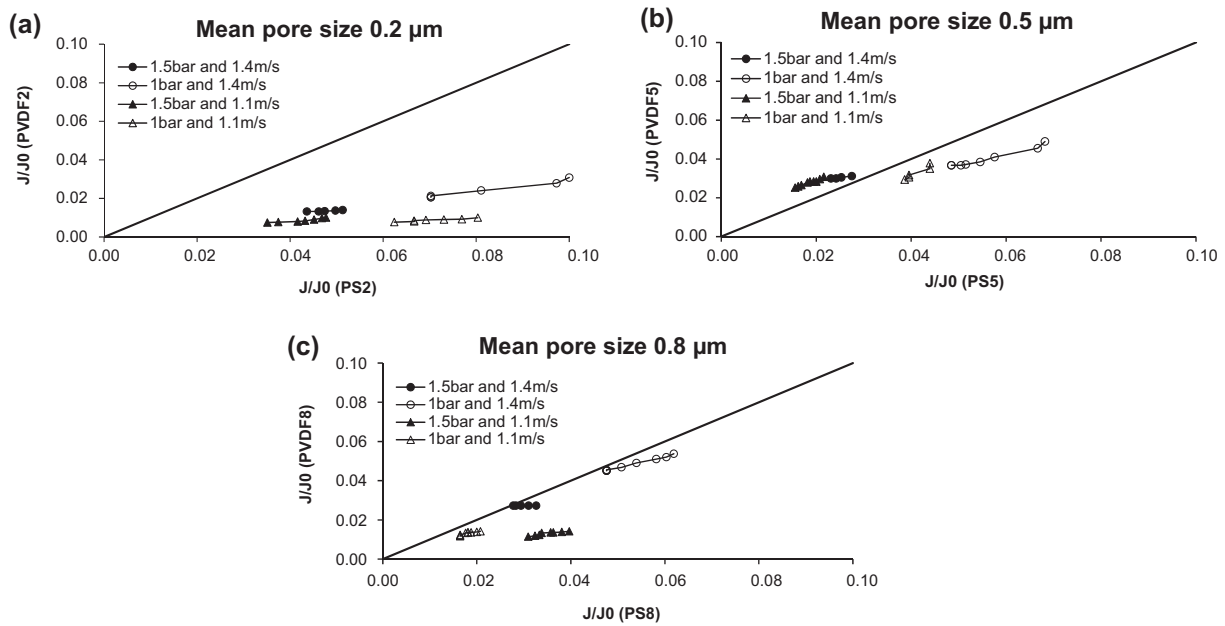


Fig. 5. Comparison of relative permeate fluxes during microfiltration. Each individual graph stands for comparison of relative permeate flux for (a) PVDF2 vs. PS2; (b) PVDF5 vs. PS5; and (c) PVDF8 vs. PS8.

For the PVDF membranes (Fig. 6), the relative fluxes were higher when using 0.5 and 0.8 μm membrane pore diameters (Fig. 6(b) and (c)) than for the 0.2 μm pore diameter membranes (Fig. 6(a)). The

increase in cross-flow velocity led to a higher improvement in relative flux for the PVDF8 membrane than for the PVDF5 membrane (Fig. 6(c)). Further, this trend is more pronounced at lower pressure than at

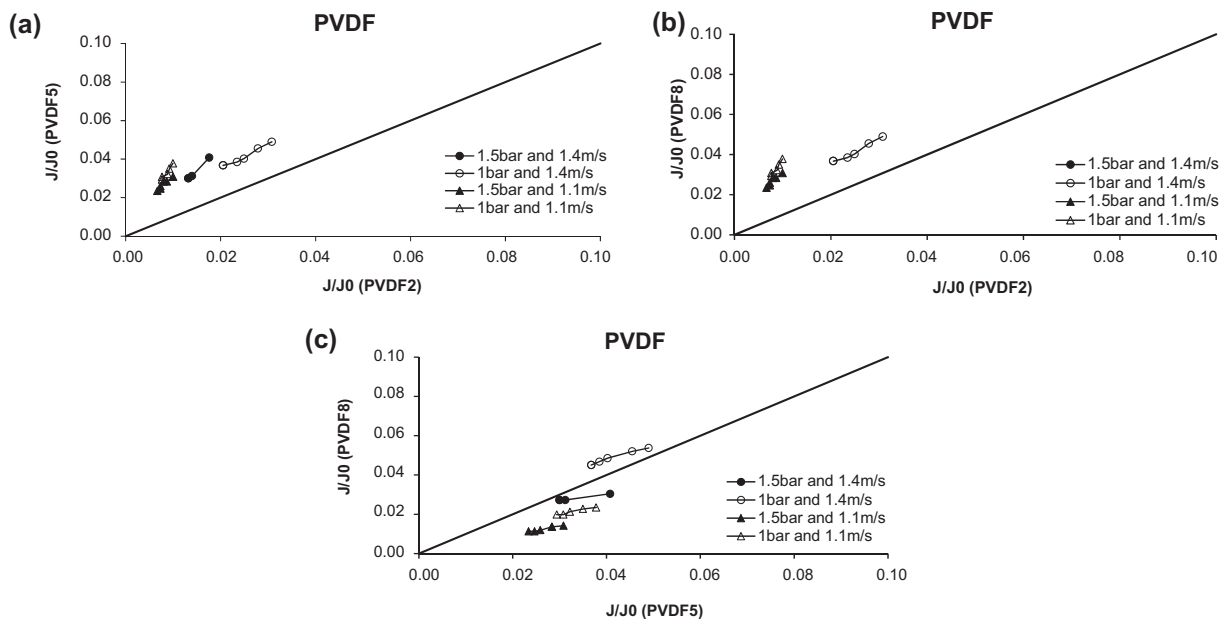


Fig. 6. Comparison of relative permeate fluxes during microfiltration considering the influence of pore size within PVDF membranes. Each individual graph stands for comparison of relative flux for (a) PVDF5 vs. PVDF2; (b) PVDF8 vs. PVDF2; and (c) PVDF8 vs. PVDF5.

higher pressure. This situation has two implications as (i) the increase in shear force, related to higher velocities, enhanced the removal of the loosely deposited particles on PVDF membranes leading to an increase in the critical flux [22] and (ii) the increase in pressure affected the relative permeate flux of the membranes more negatively on the larger pore diameters. This suggests that an increase in pressure enhances membrane blocking in the larger membrane pores of the PVDF membranes [35].

Fig. 7 shows the effect of PS membrane pore sizes on the relative permeate flux. It can be observed that the effect of material interaction was more pronounced for smaller pore sizes in PS membranes (Fig. 7(a) and (b)), especially for the experiments run at a lower pressure. An increase in pressure negatively affected the relative permeate flux on PS membranes. This most probably is due to an increasing compression in the fouling layer, especially for smaller PS membrane pore sizes (0.2 and 0.5  $\mu\text{m}$ ). In contrast, an increase in the cross-flow velocity affected the relative permeate flux of the PS membranes positively. However, this improvement was limited when compared to PVDF membranes, as foulants were strongly adsorbed on the PS membrane surfaces. The relative permeate fluxes achieved with the PS2 membranes were higher compared to the PS5 and PS8, although the relative permeate flux values for both PS5 and PS8 were very similar (Fig. 7(c)). This

suggests that for smaller pore sizes, the fouling mechanism related to PS membranes might be predominantly governed by the presence of an adsorbed layer. The adsorbed layer might increase the subsequent formation of a fouling layer for the larger pore sizes.

#### 4.2.3. Summary of microfiltration experiments

The PS membranes achieved a lower permeate flux than the PVDF membranes during, approximately, the first hour of the microfiltration experiment (shown in Fig. 4), which suggests that material interaction initially plays an important role during microfiltration of digestate liquid fractions. The lower initial permeate flux for the PS membranes could be further explained by the fact that the PS membrane surface is more hydrophobic than the surface-modified PVDF membrane [18,19]. Additionally, the PS membrane surfaces present a less-negative zeta potential (Fig. 3) than the foulants (Table 3) and, therefore, were initially more prone to foul. For the PVDF membranes, membrane and feed zeta potentials (Fig. 3) were comparable (Table 3) and, hence initially the foulants were repulsed. During filtration, as fouling builds up, the membrane zeta potential becomes less important and the similar fouling layer formed [19,36] for the two PS and PVDF membranes, limits the permeate flux behaviour. This situation shows that, although the

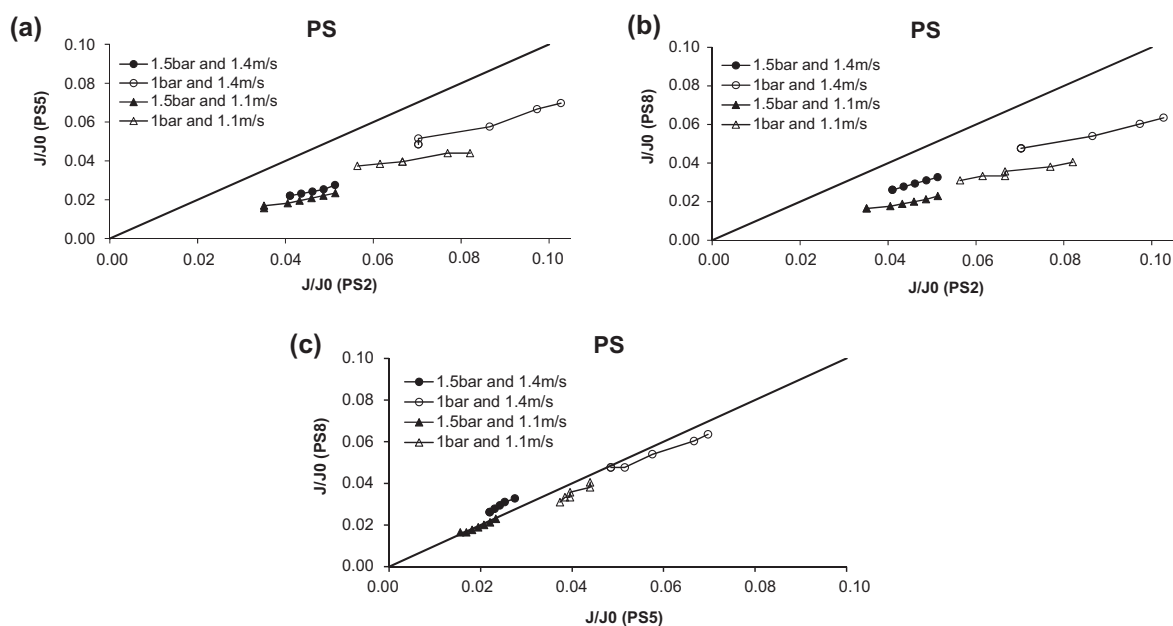


Fig. 7. Comparison of relative permeate fluxes during microfiltration considering the influence of pore size within PS membranes. Each individual graph stands for comparison of relative flux for (a) PS5 vs PS2; (b) PS8 vs PS2; and (c) PS8 vs PS5.

material interaction plays a major role at the beginning of the filtration process, the morphology and composition of the fouling layer are the dominant factors controlling the permeate flux pattern during the microfiltration of digestate liquid fractions.

#### 4.3. Microfiltration of digestate liquid fraction during concentration experiments

Batch concentration experiments were carried out on PVDF5 and PS5 membranes. During feed volume reduction, the total solid or DM concentration increased in the concentrate as well as the total phosphorus content. The volume reduction is expressed by the volume reduction factor (VRF), defined as in Eq. (2).

$$\text{VRF} = \frac{V_p}{V_0} \quad (2)$$

where  $V_p$ : Volume of permeate collected (L);  $V_0$ : Initial feed volume of feed (L).

Fig. 8 shows the relative permeate flux decline with the increasing VRF. The flux behaviour during the concentration experiments was similar to what was observed during microfiltration at constant feed concentration (Fig. 4.) for both PVDF and PS membranes at similar operational conditions ( $1.4 \text{ m s}^{-1}$  and 1 bar). For the PVDF membrane, the relative permeate flux dropped 39% when the total solids content increased from 2.3 up to 4% (Table 5). The decrease in relative permeate flux for the PS membrane was 31% when the total solids increased from 2.5 to 3.9% (Table 5). A decrease in the critical permeate flux has also been related to an increase in particle concentration [22]. In general, the flux decline during the concentration process was found to be higher for PVDF membranes than

for PS membranes as for the full recycling microfiltration experiments. This was also observed during full recycling filtration (Fig. 4) and as explained, it is the initial difference in zeta potential between the feed and the membrane material that determines the permeate flux decay pattern [12], as the initial higher resistance to fouling for the PVDF membrane is negated by a slower fouling layer build up which finally equalizes the morphology and composition of the fouling layers on the two PS and PVDF membranes.

#### 4.4. Ultrafiltration of digestate liquid fraction during concentration experiments

Ultrafiltration can be used as an alternative to microfiltration for concentration of particulate phosphorous. As an alternative, PES ultrafiltration membranes were used during the concentration experiment carried out on the Bioscan A/S (Denmark) plant for determining the capacity to reject phosphorus. Fig. 9 shows a clear relationship between the increase in the VRF together with the increase in total solids in the concentrate and the decline in permeate flux. As the total solids concentration increased, the flux decay became more acute, being reduced by more than 50% at a VRF 0.7 and 3.3 bar of applied pressure. During concentration, permeate flux decline is caused by both fouling layer build up and concentration polarization [19]. Moreover, increases in osmotic pressure could also affect the driving force for the permeate flux as the retentate concentration increases.

#### 4.5. Phosphorus rejection during concentration experiments

Fig. 10 shows the phosphorus rejection achieved with PVDF, PS, and PES membranes. The phosphorus

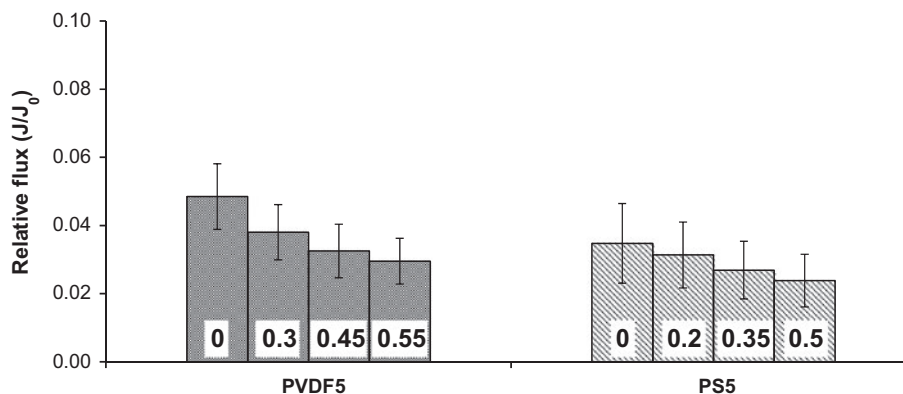


Fig. 8. Permeate flux for PVDF5 and PS5 as a function of VRF during microfiltration concentration experiments at  $1.4 \text{ m s}^{-1}$  and 1 bar (values inside the column bars indicate the related VRF for each relative flux plotted value).

Table 5

Nutrient distribution during concentration experiments using microfiltration (PVDF5, PS5) and ultrafiltration membranes (PES) (SD: standard deviation)

VRF	Membrane type	Product	DM (%)	TKN ( $\text{g L}^{-1}$ ) $\pm$ SD	TAN ( $\text{g L}^{-1}$ ) $\pm$ SD	P ( $\text{g L}^{-1}$ )	K ( $\text{g L}^{-1}$ )
0	PVDF5	Concentrate	2.3	$3.3 \pm 0.06$	$1.66 \pm 0.004$	0.148	1.32
0.26	PVDF5	Concentrate	3	$3.42 \pm 0.13$	$1.9 \pm 0.19$	0.173	1.32
0.44	PVDF5	Concentrate	4.4	$3.26 \pm 0.28$	$1.79 \pm 0.07$	0.235	1.30
0.55	PVDF5	Concentrate	4	$3.44 \pm 0.15$	$1.94 \pm 0.032$	0.275	1.37
0	PVDF5	Permeate	1	$2.50 \pm 0.05$	$2.69 \pm 0.05$	0.043	1.16
0.26	PVDF5	Permeate	0.7	$2.44 \pm 0.10$	$2.44 \pm 0.0$	0.046	1.27
0.44	PVDF5	Permeate	1	$2.60 \pm 0.14$	$2.59 \pm 0.01$	0.042	1.23
0.55	PVDF5	Permeate	1	$2.51 \pm 0.06$	$2.60 \pm 0.01$	0.039	1.27
0	PS5	Concentrate	2.5	$2.97 \pm 0.05$	$2.64 \pm 0.04$	0.213	1.47
0.18	PS5	Concentrate	3.4	$3.25 \pm 0.05$	$2.68 \pm 0.01$	0.261	1.53
0.33	PS5	Concentrate	3.9	$3.25 \pm 0.01$	$2.7 \pm 0.01$	0.291	1.40
0.48	PS5	Concentrate	3.9	$3.78 \pm 0.16$	$2.81 \pm 0.01$	0.375	1.53
0	PS5	Permeate	0.8	$2.50 \pm 0.05$	$2.69 \pm 0.05$	0.060	1.37
0.18	PS5	Permeate	0.2	$2.44 \pm 0.10$	$2.44 \pm 0.0$	0.056	1.32
0.33	PS5	Permeate	1.3	$2.60 \pm 0.14$	$2.59 \pm 0.01$	0.059	1.41
0.48	PS5	Permeate	0.9	$2.51 \pm 0.06$	$2.60 \pm 0.01$	0.059	1.41
0	PES	Feed	3.2	nd	2.7	0.53	0.46
0.7	PES	Concentrate	6	nd	2.7	0.45	0.46
0.7	PES	Permeate	0.86	nd	2.8	0.08	0.46

Note: nd—not determined.

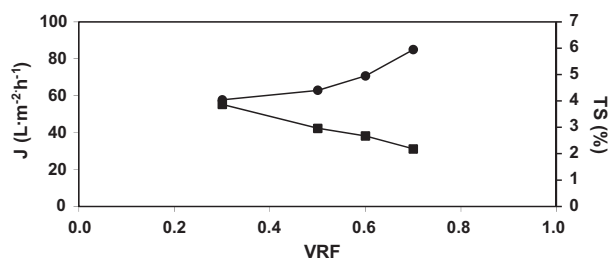


Fig. 9. Permeate flux (J) (■) and DM or total solids-% (●) as a function of VRF during ultrafiltration concentration experiments using PES 40 kDa membrane, at  $2.6 \text{ m s}^{-1}$  cross-flow velocity and transmembrane pressure 2.2 bar.

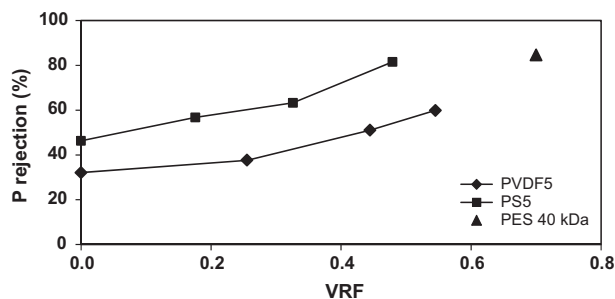


Fig. 10. Phosphorus (P) rejection in the concentrate fractions obtained during microfiltration and ultrafiltration concentration experiments.

rejection was found to be higher for the PS5 microfiltration membrane (82% w/w) than for the PVDF5 membrane (60% w/w), for the same VRF. By extrapolation, the PES membrane and the PVDF5 membrane seemed to achieve a similar phosphorus rejection. This might be another indicator that the membrane material did have a significant influence on the phosphorus rejection. Most likely a tighter fouling layer builds up on the PS membrane than on the PVDF membrane. This could lead to a higher retention of fine particles by the PS than the PVDF. A counter-argument to this explanation would be that the PES

and the PVDF show similar rejection, but as the ultrafiltration system used in this study was constructed specifically to reduce the particulate matter in principle to about 100%, the particle size distribution in the ultrafiltration feed setup was significantly different from that for the microfiltration membranes at similar VRF. It can be concluded that both the ultrafiltration setup and the PVDF microfiltration membrane achieved a comparable phosphorus rejection, although making a direct comparison of the two systems is difficult. However, microfiltration might be a cheaper treatment option.

Table 6

Clean water flux recovery (FR) after basic–acidic cleaning (compared to the clean water flux after membrane flushing)

Membrane type	Flux recovery (%) (at specific operational conditions)			
	1.4 m s <sup>-1</sup> and 1.5 bar	1.4 m s <sup>-1</sup> and 1 bar	1.1 m s <sup>-1</sup> and 1.5 bar	1.1 m s <sup>-1</sup> and 1 bar
PVDF5	20	7	17	–4
PS5	42	29	12	21

#### 4.5.1. Chemical analysis of the obtained fractions during concentration experiments

While the permeate flux decline during microfiltration and ultrafiltration concentration of digestate liquid fractions is severe, it is by no means detrimental. However, if the concentration of digestate liquid fractions is to be of practical interest, a substantial concentration of phosphorus should also be achieved. Table 5 shows the nutrient distribution between the concentrate and permeate fractions as a function of VRF. Total phosphorus is mainly attached to particles with a diameter between 0.45 and 10  $\mu\text{m}$  [9] which are mostly retained by microfiltration and ultrafiltration. Thus, as the total phosphorus content in the concentrate is directly related to the total solids content, the phosphorus concentration in the retentate increased with increasing VRF. For similar reasons, the phosphorus concentration in all permeate fractions was nearly constant during the concentration experiments. The phosphorus that could penetrate to the permeate side might be either in dissolved form or attached to particles small enough to pass through the fouling layer and membrane pores. As most of the nitrogen and potassium were present in dissolved form, the distribution of nitrogen and potassium was not affected to the same degree by the increase in total solids in the concentrate and the increase in VRF.

#### 4.6. Cleaning of fouled microfiltration membranes

Membrane cleaning was applied to recover the membrane initial permeate flux after microfiltration of digestate liquid fractions. A two-step basic and acidic cleaning procedure was tested. The basic cleaning (0.1 M NaOH, pH 12.1  $\pm$  0.1) was intended to remove organic matter, while the acidic cleaning (0.1 M citric acid, pH 2.2  $\pm$  0.1) would remove inorganic foulants. The cleaning procedures were performed after 3–4 h of microfiltration of the digestate liquid fraction. Table 6 shows the clean water flux recovery achieved after chemical cleaning compared to the clean water flux measured after the fouling cycle.

As can be observed in Table 6, the clean water flux recovery is insufficient for both fouled PVDF and PS membranes. The water flux recovery after the basic–acidic chemical cleaning was 42% for PS membranes and 20% for PVDF membranes. However, the flux recovery after basic cleaning was 19% for PS and 33% for PVDF. This indicates that the acidic cleaning might not be a good strategy for PVDF membranes. Additionally, after flushing the membranes with water, PS membranes achieved 75% of water flux recovery, while PVDF membranes reached 84%, compared to the respective final permeate flux value obtained at the end of the filtration cycle. Beier et al. [19] found that after ultrafiltration of a model of BSA solution, the initial water flux for PVDF membranes could be easily restored by flushing the membrane surface with water, while PS membranes required chemical cleaning. The reason for a better flux recovery achieved for PVDF membranes in this study could be related to the stronger attachment of the fouling layer to the PS membrane. This made the chemical cleaning of the PS membrane less efficient in recovering the initial water flux. Further investigations on PS and PVDF membranes fouled with digestate liquid fractions are necessary as the two membranes would need to undergo different cleaning strategies, rather than the ones performed in this study, to achieve higher flux recoveries as obtained elsewhere [12].

## 5. Conclusions

Two types of microfiltration membranes (PS and surface-modified PVDF), used to process digestate liquid fractions, were compared to an ultrafiltration membrane (PES) in terms of recovery of particulate phosphorus from biogas plant digestates. It was shown that the membrane material influences both the fouling mechanism and the phosphorus recovery. When comparing the two microfiltration materials used in this study, it was found that the PS membranes form a fouling layer faster than PVDF membranes but as fouling starts to build up, the permeate flux of the two membranes becomes similar. The PS membranes presented a higher initial fouling than the



PVDF membranes possibly due to a less-negative zeta potential, which tended to initially attract foulants more. On one hand, at lower pore sizes for PS membranes, the formation of an adsorbed layer seems to play the main role during fouling, while adsorption combined with a fouling layer formation seems to rule the fouling mechanism at larger PS membrane pore sizes. On the other hand, PVDF membranes reached higher permeate fluxes for larger pore sizes and the fouling mechanism is less obvious. Moreover, increases in the applied pressure affected PS membranes more negatively than PVDF membranes in terms of the relative permeate flux, most probably due to fouling layer compression, especially for smaller membrane pore sizes. Although membrane blocking could be increased with an increasing filtration pressure for larger pore sizes of PVDF membranes, increases in cross-flow velocity affected more positively the permeate flux on the PVDF membranes than the PS membranes, as foulants were adsorbed stronger on the PS membrane surface. In general, larger membrane pore sizes (i.e. 0.5  $\mu\text{m}$  and 0.8  $\mu\text{m}$  pore size) for the two PS and PVDF membranes reduced the material effect on the fouling mechanism. Additionally, it was shown that when using PS and PES membranes, a phosphorus recovery of about 80% was achieved while 60% phosphorus recovery was obtained when using PVDF membranes.

It is concluded that PS membranes could be a promising membrane material for phosphorus recovery from digestate liquid fractions, although further investigations on more suitable membrane-cleaning procedures are necessary to improve the performance of this process.

### Acknowledgments

The authors would like to thank Bioscan A/S, Fangel Biogas, and Alfa Laval Naskov for their support by providing digestate samples, facilities and scientific input, respectively. Special thanks to Mads Koustrup Jørgensen (Aalborg University) and Denis Okhrimenko (University of Copenhagen), for their guidance and input during the zeta potential measurements. Thanks to Hanne V. Hemmingsen (University of Southern Denmark) and to the Ionomic Laboratory (CEBAS, Spain) for chemical analysis of the microfiltration fractions. The research leading to these results has received funding from the People Programme (Marie Curie Actions) of the European Union's Seventh Framework Programme FP7/2007-2013/ under REA grant agreement n° [289887].

### References

- [1] M. Hjorth, K.V. Christensen, M.L. Christensen, S.G. Sommer, Solid-liquid separation of animal slurry in theory and practice. A review, *Agron. Sustain. Dev.* 30 (2010) 153–180.
- [2] R. Lopez-Fernandez, C. Aristizabal, R. Irusta, Ultrafiltration as an advanced tertiary treatment of anaerobically digested swine manure liquid fraction: A practical and theoretical study, *J. Membr. Sci.* 375 (2011) 268–275.
- [3] J.A. Alburquerque, C. de la Fuente, A. Ferrer-Costa, L. Carrasco, J. Cegarra, M. Abad, M.P. Bernal, Assessment of the fertiliser potential of digestates from farm and agroindustrial residues, *Biomass Bioenerg.* 40 (2012) 181–189.
- [4] O.F. Schoumans, W.H. Rulkens, O. Oenema, P.A.I. Ehlert, Phosphorus recovery from animal manure, *Alterra Report 2158*, Wageningen, UR, 2010.
- [5] C.A.G. Sorensen, S.G. Sommer, D. Bochtis, A. Rotz, M.L. Christensen, T. Schmidt, L.S. Jensen, Technologies and Logistics for Handling, Transport and Distribution of Animal Manures, in *Animal Manure Recycling: Treatment and Management*, John Wiley & Sons, Chichester, UK, 2013.
- [6] S. Wulf, P. Jager, H. Dohler, Balancing of greenhouse gas emissions and economic efficiency for biogas-production through anaerobic co-fermentation of slurry with organic waste, *Agr. Ecosyst. Environ.* 112 (2006) 178–185.
- [7] ECC, Directive 2000/60/EC of the European Parliament and of the council of 23 October 2000 establishing a framework for Community action in the field of water policy, in: E. Commission (Ed.), *Off. J. European Communities*, 2000, pp. 1–72.
- [8] J.B. Holm-Nielsen, T. Al Seadi, P. Oleskowicz-Popiel, The future of anaerobic digestion and biogas utilization, *Bioresour. Technol.* 100 (2009) 5478–5484.
- [9] L. Masse, D.I. Masse, V. Beaudette, M. Muir, Size distribution and composition of particles in raw and anaerobically digested swine manure, *T Asae* 48 (2005) 1943–1949.
- [10] F. Waeger, T. Delhaye, W. Fuchs, The use of ceramic microfiltration and ultrafiltration membranes for particle removal from anaerobic digester effluents, *Sep. Purif. Technol.* 73 (2010) 271–278.
- [11] K.H. Choo, C.H. Lee, U.H. Pek, U.C. Koh, S.W. Kim, J.H. Koh, Characteristics of membrane filtration as a post treatment to anaerobic digestion, *J. Korean Ind. Eng. Chem.* 3 (1992) 730–738.
- [12] X. Guo, X. Jin, Treatment of anaerobically digested cattle manure wastewater by tubular ultrafiltration membrane, *Separ. Sci. Technol.* 48 (2013) 1023–1029.
- [13] W.R. Ross, J.P. Barnard, J. Le Roux, H.A. De Villiers, Application of ultrafiltration membranes for solids-Liquid separation in anaerobic digestion systems: The ADUF process, *Water South Africa* 16 (1990) 85–91.
- [14] N.K.H. Strohwal, W.R. Ross, Application of the ADUF process to brewery effluent on a laboratory scale, *Water Sci. Technol.* 26 (1992) 95–105.
- [15] W.R. Ghyyoot, W.H. Verstraete, Coupling membrane filtration to anaerobic primary sludge digestion, *Environ. Technol.* 18 (1997) 569–580.

- [16] M.L. Gerardo, M.P. Zacharof, R.W. Lovitt, Strategies for the recovery of nutrients and metals from anaerobically digested dairy farm sludge using cross-flow microfiltration, *Water Res.* 47 (2013) 4833–4842.
- [17] B. Wu, Y. An, Y. Li, F.S. Wong, Effect of adsorption/coagulation on membrane fouling in microfiltration process post-treating anaerobic digestion effluent, *Desalination* 242 (2009) 183–192.
- [18] J. Wei, G.S. Helm, N. Corner-Walker, X. Hou, Characterization of a non-fouling ultrafiltration membrane, *Desalination* 192 (2006) 252–261.
- [19] S.P. Beier, A.D. Enevoldsen, G.M. Kontogeorgis, E.B. Hansen, G. Jonsson, Adsorption of amylase enzyme on ultrafiltration membranes, *Langmuir* 23 (2007) 9341–9351.
- [20] G. Bayramoğlu, E. Yalçın, M.Y. Arica, Adsorption of serum albumin and  $\gamma$ -globulin from single and binary mixture and characterization of pHEMA-based affinity membrane surface by contact angle measurements, *Biochem. Eng. J.* 26 (2005) 12–21.
- [21] X. Li, Y. Zhang, X. Fu, Adsorption of glutamicum onto polysulphone membrane, *Sep. Purif. Technol.* 37 (2004) 187–198.
- [22] I.H. Huisman, E. Vellenga, G. Trägårdh, C. Trägårdh, The influence of the membrane zeta potential on the critical flux for cross flow microfiltration of particle suspensions, *J. Membr. Sci.* 156 (1999) 153–158.
- [23] N. Lebolay, A. Ricard, Streaming potential in membrane processes—Microfiltration of egg proteins, *J. Colloid Interf. Sci.* 170 (1995) 154–160.
- [24] M. Nystrom, M. Lindstrom, E. Matthiasson, Streaming potential as a tool in the characterization of ultrafiltration membranes, *Colloid Surf.* 36 (1989) 297–312.
- [25] S.S. Deshmukh, A.E. Childress, Zeta potential of commercial RO membranes: Influence of source water type and chemistry, *Desalination* 140 (2001) 87–95.
- [26] A. Zarebska, D.R. Nieto, K.V. Christensen, B. Norddahl, Ammonia recovery from agricultural wastes by membrane distillation: Fouling characterization and mechanism, *Water Res.* 56 (2014) 1–10.
- [27] K. Nakamura, T. Orime, K. Matsumoto, Response of zeta potential to cake formation and pore blocking during the microfiltration of latex particles, *J. Membr. Sci.* 401 (2012) 274–281.
- [28] SurPASS Electrokinetic Analyzer, Anton Paar GmbH, 2009. Retrieved from <http://www.anton-paar.com>.
- [29] D.B. Burns, A.L. Zydney, Buffer effects on the zeta potential of ultrafiltration membranes, *J. Membr. Sci.* 172 (2000) 39–48.
- [30] K. Boussu, B. Van der Bruggen, A. Volodin, C. Van Haesendonck, J.A. Delcour, P. Van der Meeren, C. Vandecasteele, Characterization of commercial nanofiltration membranes and comparison with self-made polyethersulfone membranes, *Desalination* 191 (2006) 245–253.
- [31] A. Martin, F. Martinez, J. Malfeito, L. Palacio, P. Pradanos, A. Hernandez, Zeta potential of membranes as a function of pH—Optimization of isoelectric point evaluation, *J. Membr. Sci.* 213 (2003) 225–230.
- [32] E.W. Rice, R.B. Baird, A.D. Eaton, L.S. Clesceri, *Standard Methods for the Examination of Water and Wastewater*, twenty-second ed., American Public Health Association (APHA), American Water Works Association (AWWA), Water Environment Federation (WEF), Washington, DC, 2012.
- [33] E. Arkhangelsky, I. Levitsky, V. Gitis, Electrostatic repulsion as a mechanism in fouling of ultrafiltration membranes, *Water Sci. Technol.* 58(10) (2008) 1955–1961.
- [34] B. Razi, A. Aroujalian, M. Fathizadeh, Modeling of fouling layer deposition in cross-flow microfiltration during tomato juice clarification, *Food Bioprod. Process* 90 (2012) 841–848.
- [35] K.-J. Hwang, C.-Y. Liao, K.-L. Tung, Effect of membrane pore size on the particle fouling in membrane filtration, *Desalination* 234 (2008) 16–23.
- [36] V. Chen, A.G. Fane, S. Madaeni, I.G. Wenten, Particle deposition during membrane filtration of colloids: Transition between concentration polarization and cake formation, *J. Membr. Sci.* 125 (1997) 109–122.